Performance assessment of modelling tools for high resolution runoff simulation over an industrial site

M. Abily, C. M. Duluc, J. B. Faes and P. Gourbesville

ABSTRACT

Intense rainfall can generate storm sewer system failures along with large surface runoff events which represent an issue for industrial sites' security assessment. Numerical modelling tools, including standard bi-dimensional (2D) free surface flow models, are applied in a wide variety of flood risk practical studies straight from the purpose for which they had originally been designed. This study focuses on possibilities, performances and limits of the use of standard modelling tools for high resolution runoff simulations over an industrial site. Two categories of runoff scenarios are tested over this industrial site test case, with three modelling tools relying on different numerical schemes. Simulated water depth evolutions are found to be comparable between modelling tools, nevertheless, the possibilities of these modelling tools' optimal use with a highly refined topographical resolution for runoff scenarios are revealed to be unequal. Used indicators for computation reliability checks do not point out major inconsistencies in calculation under critical models' optimisation. Indeed, emphasis is placed on restrictive aspects to achieve with standard modelling tools a balance between computational stability, swift and precise in high resolution runoff modelling.

Key words | computation reliability check, industrial flood risk, Mike, Open FOAM, runoff modelling

M. Abily (corresponding author)
P. Gourbesville
University Nice Sophia Antipolis/Polytech'Nice-Sophia/URE I-CiTy,
930 Route des Colles,
06903 Sophia Antipolis Cedex,
France
E-mail: *abily@polytech.unice.fr*

C. M. Duluc
Institut de Radioprotection et de Sûreté Nucléaire (IRSN),
PRP-DGE, SCAN,
BEHRIG, BP17,
92 262 Fontenay-aux-Roses Cedex,
France

J. B. Faes
Néodyme,
63 boulevard Sébastopol,
75001 Paris,
France

ABBREVIATIONS AND NOTATION

2D	Bi-dimensional
3D	Tri-dimensional
BB	Building block method
BH	Building hole method
CFL	Courant–Friedrich–Lewy number
CFL_{max}	Maximal Courant–Friedrich–Lewy number
DEM	Digital elevation model
DHI	Danish Hydraulic Institute
FVM	Finite volume method
h_{init}	Initial condition for water depth
h_{max}	Maximal water depth
h_{wet}	Threshold for complete SWEs resolution in Mike
LiDAR	Light detection and ranging
NSE	Navier–Stokes equations
S1	Rainfall scenarios
S1a	Constant intensity rainfall scenario
S1b	Triangular intensity rainfall scenario
S2	Initial 10 cm water depth scenario
S_g	Ground surface cell
SWEs	Shallow water equations
T_c	Concentration time
T_{lag}	Lag time
UAV	Unmanned aerial vehicle
U_{max}	Maximal flow velocity
V_{cell}	Volume of fluid in a cell
VOF	Volume of fluid

BACKGROUND

An industrial site generally covers a few square kilometre area in a platform or a sub-catchment-like configuration. Sites are characterised by a highly dense presence of above-ground infrastructures (building, walls, road-curbs,

doi: 10.2166/hydro.2013.063

pavements, etc.). It creates a complex environment with small-scale surface flow obstacles greatly influencing drainage paths. Water intrusion within an industrial facility can result in serious consequences and flood risk assessment becomes a key issue for industrial sites conducting sensitive activities (e.g., in the case of nuclear activities).

Over the last two decades, deterministic surface flow numerical models have been widely used for flood risk studies at a large range of scales. The increasing use of models based on the bi-dimensional (2D) shallow water equations (SWEs) is observed in practices for surface runoff component modelling in urban areas (Ettrich 2005; Ciliberti *et al.* 2008; Gomez *et al.* 2011). In parallel, modern techniques for high resolution topographical data gathering are becoming commonly used in practical engineering studies. The density and complexity of above-ground structures on industrial sites, as well as their effects on drainage paths, justify the use of high resolution methods to assess properly the runoff risk on such an environment.

Consequently, the need of expertise for industrial flood risk evaluations may result in the use of standard modelling tools in practical applications for intense runoff survey using high resolution topographical data. In this context, the use of standard 2D modelling tools for runoff modelling for industrial sites deserves special consideration. This being the case, it appears essential to address the reliability of the use of these practical tools for such a purpose. Indeed, for an industrial site environment, intense runoff might result in rapid changes in flow regime, small water depths and high gradient properties. Numerical treatment of these properties by standard 2D SWEs-based models could become challenging. Indeed, if standard 2D SWEs-based models application domain boundary is reached this might lead to restrictions for their use.

Some of the above-ground components of industrial environments (e.g., walls, sub-platforms, etc.) introduce vertical effects in runoff hydrodynamics. Even if their impact seems negligible compared to the overall horizontal dimensions of the physical runoff process, tri-dimensional (3D) numerical models have been tested. Indeed, this category of modelling tools is extensively used by consulting companies working with industries for other categories of safety assessment purpose. Therefore, industrial operators might end up using this category of modelling tools to demonstrate the safety of their installation regarding runoff risk.

The aim of this paper is to focus on commonly used standard numerical modelling tools' performances to calculate surface runoff water depth evolutions over an industrial site test case, in a storm sewer system failure context. The objective is also to assess the possibilities and limits of high resolution topographical data use with different categories of standard numerical modelling tools.

To examine the feasibility, performances and limits of such an approach, two categories of scenarios with equal quantities of water in the context of a blocked stormwater sewer system were tested:

1. A 1-h long rainfall event totalling 100 mm, according to two different temporal distributions (S1a and S1b).
2. An initially 0.1 m high water elevation over the whole domain (S2).

Even if equal quantities of water are considered, these two scenario categories lead to different runoff dynamics and their simulation may highlight different kinds of critical modelling aspects to monitor.

The work presented here is based on a test case which has specificities of real industrial sites in terms of spatial extent, topography and infrastructures that influence surface drainage paths.

The selected standards modelling software belong to three different categories of modelling tools widely used by consulting companies in practical engineering applications:

- Danish Hydraulic Institute (DHI) 2D SWEs finite difference and volume-based hydrodynamic modules, respectively Mike 21 and Mike 21 FM (DHI 2007a, b).
- An OpenFOAM (distributed by OpenCFD Ltd) based tri-dimensional finite volume method (3D FVM), using pre- and post-processing tools developed by Néodyme Company.

The objective of the analysis is to assess the performance, limits and added value of each modelling tool in a test case where the runoff dynamic, especially in the light of water surface elevation, has to be evaluated with a high degree of accuracy.

TEST CASE ELABORATION

Industrial site digital elevation model (DEM)

The topographic modelling is a key issue, especially when the objective of the analysis is to address high-definition processes like flooding of footpaths and intrusion into buildings (Gourbesville *et al.* 2004). Previous experiences (Gourbesville *et al.* 2004; Gourbesville 2009) have clearly demonstrated the importance of an accurate representation of the geometry. In complex environments like urban or industrial areas, details have to be carefully modelled and integrated into the DEM. A significant part of the quality of the model is driven by the quality of the DEM.

The baseline for the test case was to develop a representative industrial site's topographic configuration. Infrastructures and constructions considered in the test case domain are: buildings, banks, walls, roads, pavements, curbs and door steps. A slight slope over the constructed area, orienting the drainage path to drainage structures, is included as well (Figure 1). The roof area contribution to the surface runoff was included using source points representing gutter discharges. The spatial extent of the test case is about 65,000 m^2. Possible upstream surface runoff from outside the represented domain is assumed to be drained by an outer natural and artificial drainage system beyond the boundaries of the domain.

To achieve a horizontal topographical resolution accurate enough to represent flow influencing structures in urban areas, the interval of spot elevation data should be in the range of 0.1–0.4 m for DEM generation (Mark *et al.* 2004). This order of magnitude in DEM resolution is consistent with modern geomatic technologies for spatially dense topographical data information gathering like unmanned aerial vehicle (UAV) photogrammetry (Remondino *et al.* 2011) or aerial light detection and ranging (LiDAR) among others (Ettrich 2005; Aktaruzzaman & Schmidtt 2009; Tsubaki & Fujita 2010). Thus, a DEM was created with a 0.1 m cell size resolution. This grid resolution fits with the required horizontal precision to represent the above-mentioned infrastructures.

Runoff scenarios

The two approaches considered for surface runoff modelling scenarios introduce the same quantity of water over the domain with a homogeneous spatial repartition.

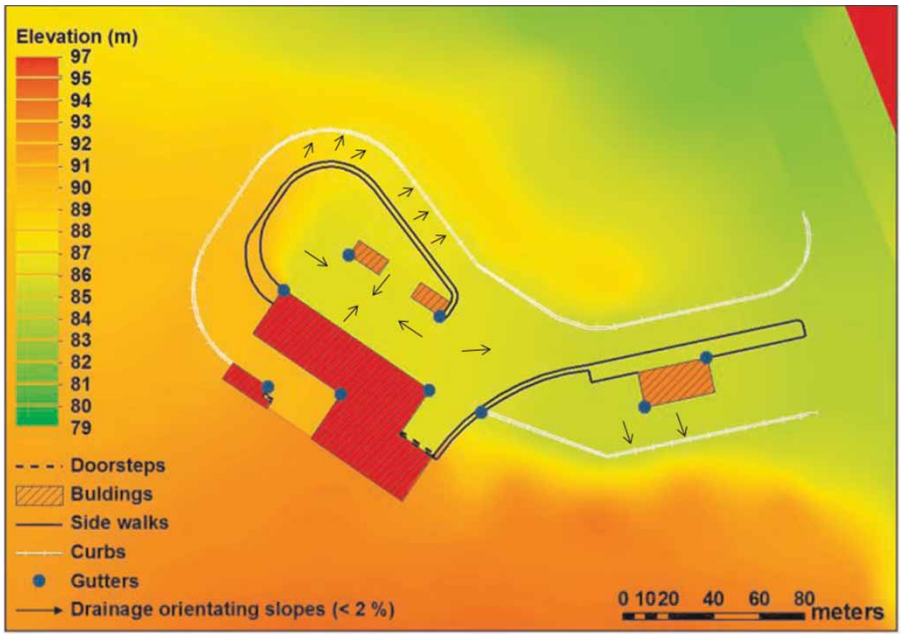

Figure 1 | Infrastructures represented in the test case.

- The first category of scenario (S1) is based on a 1-h-long rainfall event totalling 100 mm. Two cases were envisaged (Figure 2), one with a constant rainfall intensity-100 mm h^{-1} (S1a) and one with a triangular intensity variation over the event duration (S1b).
- The second scenario category is based on an initial 0.1-m-thick water surface elevation over the entire industrial site domain (S2).

These two categories of scenario were not compared with each other in detail as they do not have comparable physical meaning. Nevertheless, both approaches deserve to be considered to show the models' applicability, performances and limits.

For S1a and S1b, the overland flow was simulated for up to 1 h after the end of the rainfall event. For S2, overland flow was simulated for 30 min.

MODELS' DESCRIPTION

Selected modelling tools

The three modelling softwares tested for our study are: Mike 21, Mike 21 FM and Néodyme's 3D FVM. Pre- and post-processing tools used with Mike 21 and Mike 21 FM are those included in DHI software package, whereas specific meshing tools have been developed by Néodyme's R&D team for 3D FVM. Detailed industrial topography created includes flow obstacles which may lead to rapid changes of flow conditions (e.g., flow regime change, hydraulic jumps, flood waves, etc.). As 2D SWEs are hyperbolic differential equations, mathematical discontinuities, represented by these rapid flow changes, can be treated by these equations under certain conditions (Liang *et al.* 2006). A fully 3D model can compute solutions for these flow specificities requiring heavy geometrical construction and meshing workload.

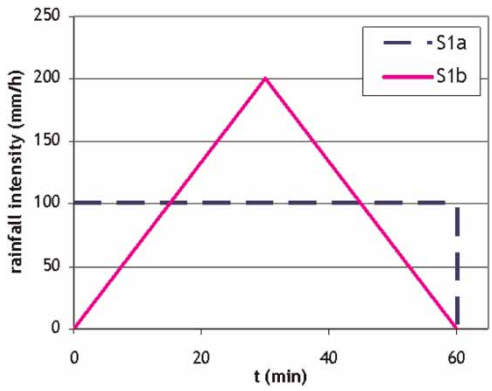

Figure 2 | S1 types of rainfall events.

Mike 21 is based on the resolution of 2D SWEs. The mass conservation equation and the set of two Cartesian coordinate momentum equations are solved using finite difference approximation on a regular grid (DHI 2007a). This category of numerical method, when satisfying specific conditions, has the ability to handle previously mentioned numerical discontinuities (Lax & Wendroff 1960; Liang *et al.* 2006). Mike 21 code uses an alternate direction implicit (ADI) method to resolve SWEs (DHI 2007a). Usually, ADI methods are not considered to perform well in the case of trans-critical flow occurrence (Meselhe & Holly 1997; Madsen *et al.* 2005; Liang *et al.* 2006). Nevertheless, modifications have been implemented in the Mike 21 ADI scheme by DHI, as presented by McCowan *et al.* (2001), switching from central to up-wind treatment of the convective terms of momentum equations in the case of change from infra to supercritical flow. This method adds a selective numerical dissipation in the case of supercritical flow, thereby reducing spurious numerical oscillation, and therefore increasing the calculation stability but locally reducing its precision.

Mike 21 FM is based on 2D SWEs resolved on a flexible mesh with a Godunov spatially centred finite volume scheme. An approximate Riemann problem solver (Roe) is used to calculate convective fluxes at each cell interface. Time integration is a first order Euler method (DHI 2007b). This category of scheme has been tested in many applications and can numerically handle treatment of discontinuities. A TVD (total variation diminishing) slope limiter and Runge–Kutta time integration are solver options available and tested with the software.

The 3D FVM (Versteeg & Malalasekera 2007) is based on the NSE solved under their integral form. This method requires the subdivision of the computational domain into elementary volumes (the cells). Numerical resolution of the NSE in each cell is carried out by using the OpenFOAM suite (Hrvoje 1996). OpenFOAM is an open source

computational fluid dynamic code containing C ++ libraries designed to solve systems of partial differential equations encountered in fluid dynamic fields (among others). From this OpenFOAM code library, the solver 'interFoam' was used for this study (Henrik 2002). This solver is based on the volume of fluid (VOF) method (Gopala & Wachem 2008) which requires the resolution of equations of conservation for the two considered phases (air and water). The fluids' physical properties are thus calculated from the volume fraction of each fluid in each cell. Near the water surface, the air–water interface is not marked by a sharp discontinuity. Thus, the modelling of the liquid surface is enhanced by an artificial interface compression term. This solver use has proved to be very efficient in simulating free surface flow, for cases where the fraction of liquid in the domain is not negligible. In the present case, a very narrow layer of water covers the ground of a large environment. That is not a standard case, and the solver method performance depends on the ground surface mesh 3D resolution.

Models' general parameters

Boundary conditions

With all the selected modelling tools, the general purpose was to set boundary conditions close and far enough from the area of interest so that they do not interfere with flow in this area. Over the domain, initial condition for water depth (h_{init}) and velocities were null for scenarios S1a and S1b, whereas for S2, h_{init} was equal to 0.1 m and velocities equal to 0.

In both Mike 21 and Mike 21 FM software, a cell is either considered as a part of the solution domain (wet) or as a boundary (dry) (DHI 2007a, b). A threshold value (h_{dry}) represents the boundary value under which water can be accumulated, but 2D SWEs are not resolved. 2D SWEs are fully resolved when a cell water depth is above a user-defined threshold value (h_{wet}). Between h_{dry} and h_{wet}, only a part of the 2D SWEs are resolved. For the purposes of this paper, we are interested in the full resolution of 2D SWEs and therefore a minimisation of these thresholds in models' setup has been performed. Thus, only water levels above h_{wet} are analysed. The 3D FVM is able to capture any small height of water.

Spatial discretisation

The selected modelling tools use different numerical schemes and notably, different spatial discretisation approaches (Figure 3). The mesh structure and resolution play an important role in models' performance and stability.

In Mike 21, models' DEM grids can be used for discretisation whereas with Mike 21 FM, non-structured mesh was generated to discretise the domain with an important refinement in order to finely represent flow influencing infrastructures. In addition, two approaches for building representations were used. In Mike 21, buildings were represented as elevation data (building block method: BB). In Mike 21 FM, buildings were excluded from mesh using their footprints as break lines. In that case, a normal no-slip wall boundary condition was applied to account for the blockage effects of buildings (building hole method: BH). For urban flooding simulations, these approaches equally fulfil requirements for building representation to

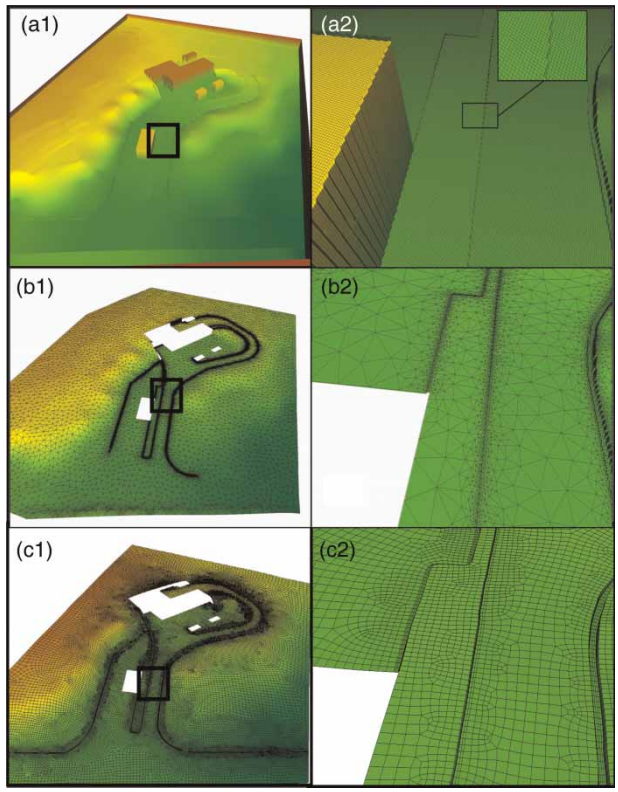

Figure 3 | Mesh used in models (where: a1, a2 are Mike 21 grid views; b1, b2 are Mike 21 FM mesh views; c1, c2 are Néodyme 3D FVM mesh views).

predict flood extent (Schubert *et al.* 2008). For the S1 scenario category, rain over the roofs of buildings is included in the models' calculations through source points representing gutter discharges. Gutter discharges are assumed to be constant during rainfall events. Each gutter discharge is established simply by calculating contributing cumulated roof rainfall volume and dividing it by length of rainfall event. Calculated gutter discharges range from 0.0015 to 0.01 $m^3 s^{-1}$.

In the 3D FVM case, the chosen meshing method mainly consists of extruding surfaces meshed with quadrilaterals by use of the Q-Morph algorithm (Owen & Saigal 2000). Powerful meshing tools have been developed by the Néodyme's R&D team and incorporated into the *gmsh* meshing software (Geuzaine & Remacle 2009), allowing the discretisation of complex environments consisting of a topographical terrain and urban structures. An adaptive distribution of layers links the natural ground surfaces and urban structures to a horizontal flat surface, later assimilated to the atmosphere. For numerical treatment, the 10 cm resolution raster is put in memory by extensive use of octrees, giving rapid access to the topography during mesh manipulation. Urban structures represent discontinuities in the topography that cannot be extruded. The points located near these strong gradient zones are first extracted from the original raster, and then collapsed along geometrical curves fitting the actual geometry. Finally, these lines are used to draw local 3D structured volume meshes with *gmsh*. These volumes are grouped into two categories: 'channels' (hollow) and 'side mounts' (elevations). Remaining areas consist of a continuous topography. This process is summed up in Figure 4. Finally, the goal is to build a surface covering the entire domain (including channels and mounts) sufficiently continuous to be extruded. In order to avoid a prohibitive number of cells in the final mesh, the resolution is progressively degraded far from the discontinuities.

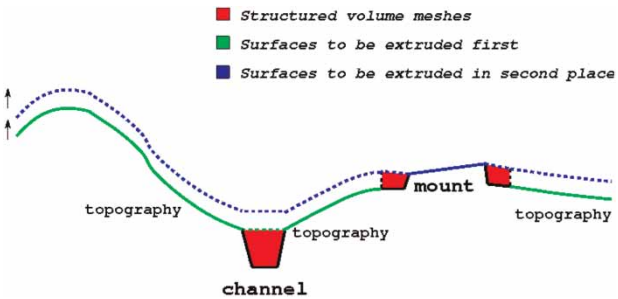

Figure 4 | Illustration of the method used to construct the final volume mesh for FVM used by Néodyme.

Energy loss parameters

For Mike 21 and Mike FM models, a Manning's M roughness coefficient value of 60 $m^{1/3} s^{-1}$ was applied in a constructed area. In a non-constructed area, its value was fixed to 27 $m^{1/3} s^{-1}$. For energy losses due to horizontal turbulence, the Smagorinsky eddy viscosity approach, which is a function of velocity gradient, was used in Mike models. A constant Smagorinsky coefficient of 0.28 was used. For Néodyme 3D FVM, the Reynolds average stress (RAS) approach is used for turbulence modelling, and the *k*-omega-SST turbulence model (Menter 1993) has been chosen. Small scale details under grid cell size are taken into account effectively through the 'equivalent sand-grain roughness height' (Nikuradse 1933) whose acceptable values are taken to be 1 and 3 cm for urban and natural surfaces, respectively.

PERFORMANCE ASSESSMENT METHODOLOGY

The parameter of interest in modelling results was the maximal water depth (h_{max}) calculated by models for each scenario. Indicators for computation reliability checked are listed here. Indeed, even though used models are conservative, errors in mass might be numerically induced and mass balance was therefore checked. In general, mass errors might happen due to the initial flooding cycle, to flooding and drying scheme, to a high gradient in topography or to a large time step use (McCowan *et al.* 2001). In addition, maximum Courant numbers (CFL_{max}) reached in simulations were checked to look for potential numerical instabilities in models as well as for calculation accuracy purposes. Maximal velocities (U_{max}) as well as hydrograph characteristics' time results were observed to check their coherence with physics of modelled phenomena. Velocity field evolutions were analysed to detect any artificial polarisation.

Framework for models' comparison

Optimised setups for each modelling software and scenarios were defined. Indeed, to obtain stable and comparable models, several setup tests were carried out. The purpose was to model scenarios using optimal parameters and to obtain balanced computation and runs with regard to: objectives, model possibilities and computer performances. For the study purposes, standards considered as optimal were:

- a fine discretisation use;
- a minimisation of complete SWEs resolution threshold;
- a non-prohibitive computational time.

The computational resources used were a desktop computer (Intel Core2 Duo Processor E8400) for Mike 21 and Mike 21 FM model runs. A set of 10 processors (Two Intel Xeon X5680) of a Linux workstation was used to perform the 3D finite volume calculation.

Possibilities in reaching a balanced model setup for our specific applications were compared.

Optimisation of models' setup

Depending on models' optimisation possibilities and limitations, differences in parameterisation were generated. Table 1 summarises the optimal setup reached for each model that was considered for comparison.

With Mike 21, all categories of scenarios could be computed but the 0.1 m resolution DEM grid used as mesh for discretisation did not lead to stable runs. This resolution use would have probably been possible through a time step reduction, but this software release did not have a time step smaller than 0.01 s. It limits calculation stability for such a fine spatial discretisation use. Therefore the 0.1 m resolution grid has been degraded to a 0.3 m resolution grid which was used for discretisation. The selected h_{wet} value is 0.008 m as for higher values, with tests showing important spurious oscillations leading to a poor quality result. Here, computation time was about 72 h for S1a and S1b scenarios and 24 h for S2 scenario runs.

Mike 21 FM could not perform the S2 scenario run. The use of higher order scheme options was not conducive to stable runs. Neither was it possible to obtain stable runs with a h_{wet} value smaller than 0.02 m for S1a and 0.025 m for S1b. Computation time was about 140 h for S1a and S1b scenarios. Moreover, in the case of high topographical gradients, calculation stability could not be maintained in models. Therefore, BH treatment of a high wall was applied to remove it from calculations and allow stable runs.

Néodyme's 3D FVM could not model the S1 category of scenario, as options to implement such a kind of approach are still under development. For the S2 category of scenario, vertical structures such as walls generate high gradients in flow and had to be removed from the simulated domain for the sake of computation stability. Computation time was about 530 h here.

RESULTS

This section presents the parameters of interest (h_{max} and water depth evolution) and the computation reliability indicator results. It has to be remembered that S1 and S2 categories of scenarios do not have comparable hydrodynamics and the results of their comparison *stricto sensus* is not the purpose of this paper. Nevertheless, separately they can give an insight into modelling tools' limits and flexibility. The results comparison in the light of (i) the approach specificity, (ii) the different numerical schemes' properties and (iii) the optimisation possibilities will be dealt with in the 'Discussion' section.

Rainfall events scenarios (S1)

Maximal water depth (h_{max})

A general overview of h_{max} values calculated for rainfall scenarios (S1a and S1b) with Mike 21 and Mike 21 FM models is presented in Figure 5. Within the constructed zone of the study domain, all models and scenarios estimate the same four flooded areas (A to D) with a calculated h_{max} value ranging from 0.05 to 0.15 m. Identified flooded areas have the following topographical configurations:

- Area A is a depression, not connected to any surface drainage structures but the crest line of the depression, leading to a unique drainage path.
- Area B is a corner between a building and a sidewalk.

Table 1 | Setup of models used for comparison of results

		Scenarios		
Modelling software	**Main parameters**	**S1a**	**S1b**	**S2**
Mike 21	Numerical scheme	Finite differences, ADI		Finite differences, ADI
	Grid resolution	0.3 m × 0.3 m (based on 0.1 m resolution grid)		(Interpolated based on 0.1 m resolution grid)
	Number of cells	718,200		718,200
	Dt (fixed)	0.01 s		0.01 s
	Boundary conditions	Closed		Closed
	Initial condition	0 m		0.1 m
	Wetting/drying threshold	0.008 m		0.008 m
	Flow evacuation	Sink		Reservoir
	Building representation	Building block (elevation data)		Building block (elevation data)
	Source point	Gutter		No
Mike 21 FM	Numerical scheme	Finite volume, (Roe solver and Euler explicit)		Not stable
	Flexible mesh	Based on 0.1 m resolution grid		
	Number of elements	87,700		
	Elements area information	Minimal: 1×10^{-5} m^2		
		Maximal: 7.99 m^2		
		Average: 0.5 m^2		
	Dt (varying)	0.1–10^{-12} s		
	Boundary conditions	Closed		
	Initial condition	0 m		
	Wetting/drying threshold	0.02 m	0.025 m	
	Flow evacuation	Sink		
	Building representation	Building hole		
	Source point	Gutter		
Néodyme 3D FVM	Numerical scheme	Not possible to implement yet		Finite volume (mixed explicit schemes)
	Mesh			Non-uniform hex-dominant
	Number of cells			697,262
	Dt (varying)			10^{-3}–10^{-2} s
	Boundary conditions			Closed everywhere but top-side open to the atmospheric condition
	Initial condition			0.1 m
	Wetting/drying threshold			0 m
	Flow evacuation			Reservoir
	Building representation			By extrusion and partially structured mesh
	Source point			No

- Area C is a narrowing roadway, lined on one side by a pavement and on the other side by a flooded curb.
- Area D is a parking zone with a slight slope (about 2%).

The h_{max} values and spatial extent of flooded areas A to D are coherent with their topographical and drainage path configurations. For a given scenario, Mike 21

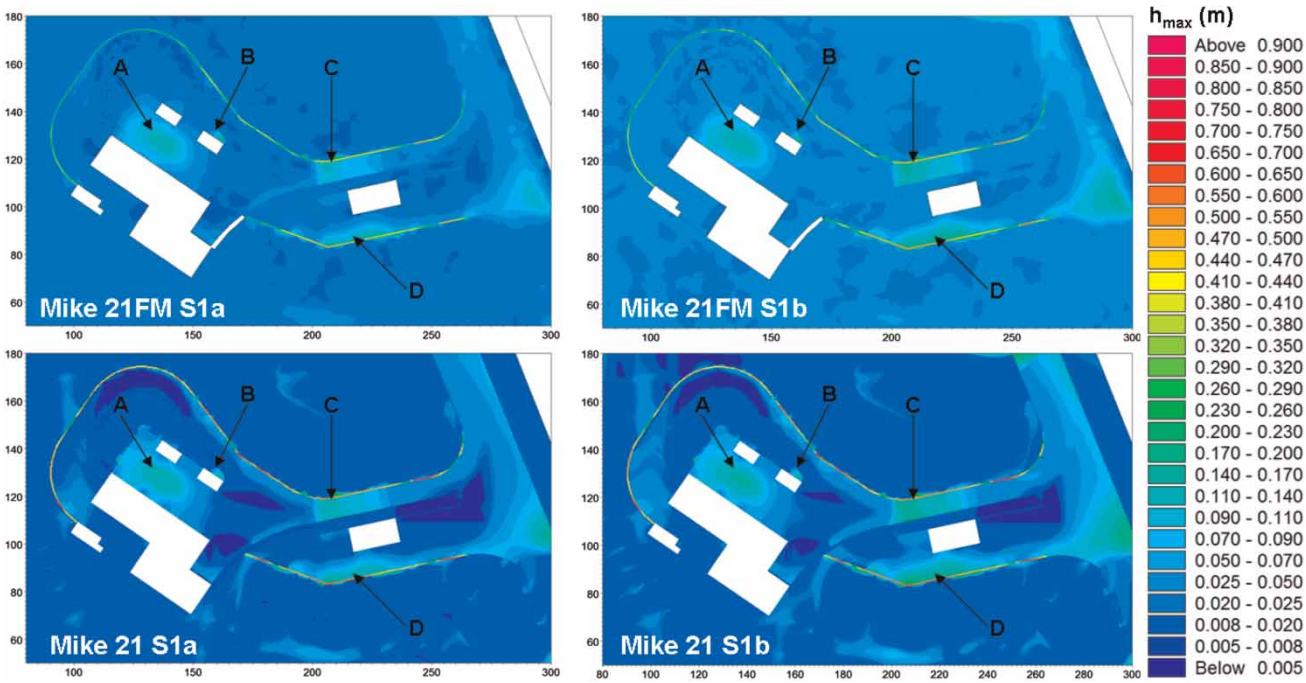

Figure 5 | Maximal water depth (h_{max}) values reached in cells for S1a and S1b scenario simulations with Mike 21 and Mike 21 FM.

and Mike 21 FM models, computed h_{max} values had close values and the flooded area had a similar spatial extent.

The comparison of scenarios S1a and S1b results shows that h_{max} values in flooded areas were up to 0.06 m higher for scenario S1b than for scenario S1a, representing a maximal difference in h_{max} value among scenarios of up to 30% in these areas. S1a and S1b flooded areas' spatial extent with h_{max} values greater than 0.05 m were compared. S1b led to a 15% (with Mike 21) and to a 24% (with Mike 21 FM) increase of flooded areas' spatial extent.

A more detailed comparison of calculated h_{max} values was carried out for 18 points of interest throughout the industrial site, showing an average difference in results between Mike 21 and Mike 21 FM models of 0.01 m for S1a and 0.012 m for S1b. Computed h_{max} values for 10 of these points of interest are presented in Figure 6. Point 1 is located at the lowest point in the middle of flooded area A. Points 3 and 4 are located at the entrance to two buildings in flooded area A (Figure 5). Points 6 and 7 are, respectively, located above and below a 0.15 m high doorstep which was not flooded and with no upstream contributing area. Therefore, h_{max} values at point 6 are equal to the models' respective parameterised h_{wet} values. The same applies to point 10 located on a non-flooded pavement. Points 11 and 12 are located on a flooded road (area C); observed h_{max} values for point 12 are equal to a close by pavement relative elevation, which was nonetheless not flooded. Point 18 was located in flooded area D (Figure 6).

Mesh resolution difference can be important, and as the h_{max} value is averaged over a cell area this might lead to differences. For instance at point 18, Mike 21 regular mesh cell area is 0.09 m^2 whereas Mike 21 FM cell size at this location is about 2 m^2.

Water depth evolution

From a general perspective, for a given scenario, Mike 21 shows agreement with Mike 21 FM in calculation of water depth evolution on the area of interest. Figure 7 illustrates the water depth evolution comparison at point 18 where differences in h_{max} calculation are important.

Scenarios S1a and S1b differences in rainfall intensity evolution resulted in differences in water depth evolutions. Moreover, differences in water depth evolution in the first minutes of simulations are spotlighted in Figure 7. These differences are related to models' differences in h_{wet}

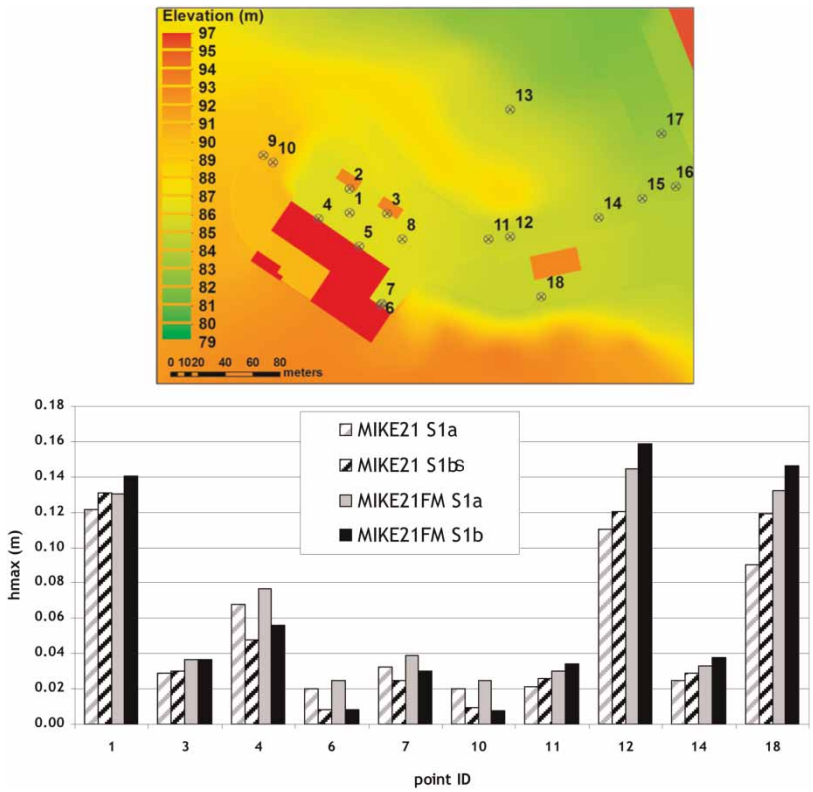

Figure 6 | Detail of h_{max} values at 10 specific points of interest (lower) and points location (upper).

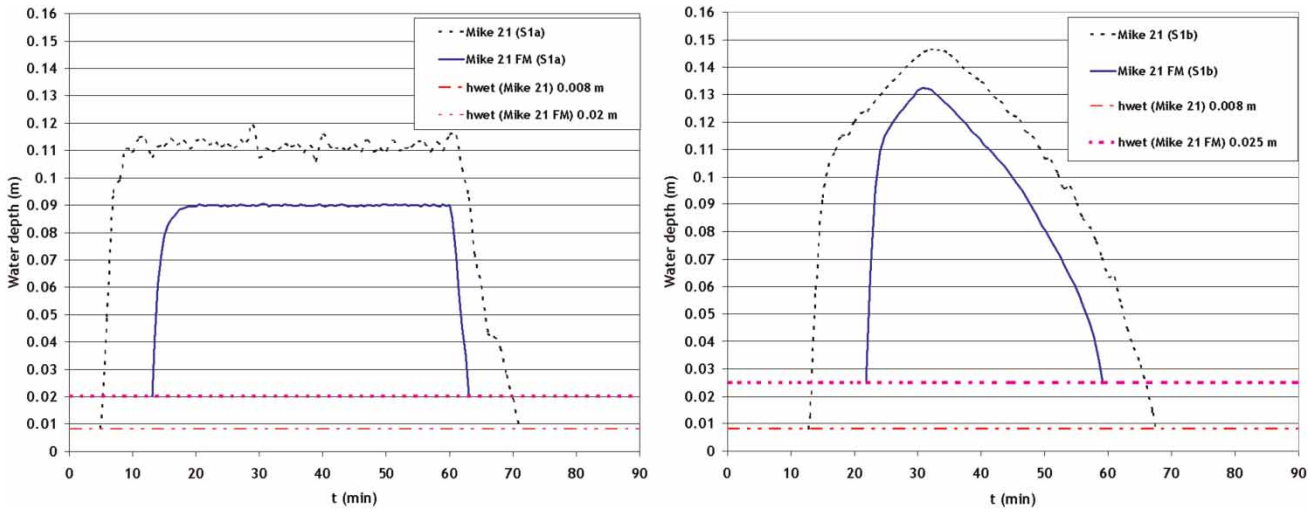

Figure 7 | Water depth at point 18 with Mike 21 and Mike 21 FM, for scenarios S1a (left) and S1b (right).

values. Indeed, 2D SWEs are not fully resolved over the whole domain until accumulated rainfall value exceeds h_{wet}. Below h_{wet} value, water in a cell is either considered as not moving (if below h_{dry} value) or only mass flux momentum SWEs are resolved (if between h_{dry} and h_{wet} values). As h_{wet} value was optimised to 0.008 m (with Mike 21) and to 0.02 m (with Mike 21 FM) for S1a, and to 0.008 m (with Mike 21) and 0.025 m (with Mike 21 FM)

for S1b, the times for accumulated rainfall to exceed h_{wet} are respectively 5 min, 12.5 min and 12 min and 21.75 min.

Global water depth evolution is shown to respond quickly to rainfall event temporal variations due to configuration (sloppy) and to size of the modelled area. For instance, h_{max} at point 18 was observed about 3 min after the peak in S1b rainfall intensity which occurs at 30 min.

Even though compared to Mike 21 FM, Mike 21 model water depth values and evolutions are comparable, they present slight spurious oscillations. These numerical oscillations are due to the fact that Mike 21 uses a fixed time step in calculations for temporal discretisation. Indeed, in both models, numerical discretisation cannot properly handle compatibility between numerical flux and source term. Nevertheless, the flexible time step used by Mike 21 FM tends to reduce magnitude of these oscillations.

Initial 0.1 m height water depth scenario (S2)

This section is devoted to the comparison of the results obtained with Mike 21 and those obtained with OpenFOAM for scenario S2. Global effects are summarised in Figure 8, showing the maximum water depth reached at each point of the domain during the entire simulation. A global agreement for maximal water depth values and repartition with the two models can be observed. Differences occur locally notably at the foot of the right hand side building (Figure 8) and in more downstream areas. These differences are up to 0.1 m and mainly due to heterogeneities between models in topography representations, velocity calculations and numerical schematisations, as discussed below.

Dynamic aspects can be more finely compared on limnigraphs (Figure 9), and especially in the area of congestion located downhill on the right, where point 14 lies. High hydrodynamic flow effects and maximal water depth phenomena occur during the first 30 s of the simulations. From $t = 0$ s to $t = 20$ s, three peaks occur successively, corresponding to direct arrival of water flowing respectively from close to the pavement, bank and road. Arrival times and magnitudes of these peaks differ between models. The main water height peak starts at $t = 25$ s and corresponds to the arrival of water from the upstream area. The

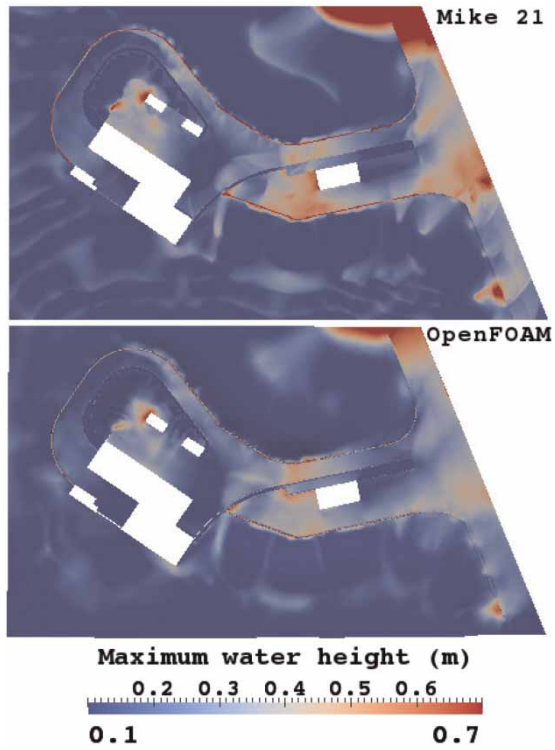

Figure 8 | Maximal water depth (h_{max}) reached over the domain for S2 scenario simulations.

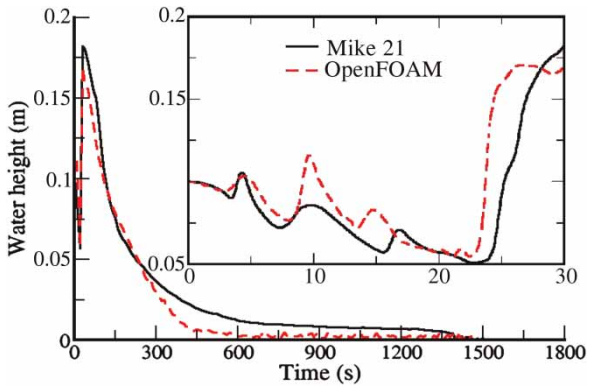

Figure 9 | Limnigraph at point 14.

slope observed around 25 s on the limnigraph shifts and appears sooner in the OpenFOAM simulation, and then the water height diminishes faster than in the Mike 21 simulation. In the Mike 21 simulation, the computational domain is drained after 30 min and only a few puddles remain after this time. The OpenFOAM

simulation also ran for 30 min but the domain was emptied sooner.

The above-mentioned differences between the two models have three main origins explained as follows.

First, the meshing method can alter the topography. The meshing tool developed by Néodyme projects a quadrilateral mesh onto the topography, and then unwraps the skew cells (Bidmon & Thomas 2005). This unwrapping procedure locally affects the original topography. This results at global scale in smoothing of the topography, reducing small topographical irregularities. Beside geometrical aspects, grid cell size resolution is finer at the ground level with Mike 21 compared to the Néodyme model as the number of cells is 718,200 in the Mike 21 regular grid, whereas the number of cells is 697,262 but for 14 layers in the Néodyme 3D FVM. Up to a certain point, larger cell size might speed up mass transfer computation and therefore influence results. That explains why the downhill accumulation of water is less pronounced in the OpenFOAM simulation, and why the domain is emptied sooner.

Next, the roughness definition leads to differences in the velocity field. Indeed, roughness parameters were separately evaluated in each model, and their conformity is not guaranteed (this would need a study in itself, and is not the purpose of our paper). Indeed, the higher the water velocity flowing downwards over the bank, the faster the fluid flow when impacting curbs and pavements, thus the more important might be the water quantity passing above them. Moreover, these structures' overflow phenomena can be more accurately represented in the Néodyme 3D FVM model as the vertical velocity flow component occurring in such a situation is considered in this model.

Finally, with Mike 21, the mesh is a regular grid directly taken from the raster. It leads to a stairs-shaped representation of urban structures. This limitation is inherent to regular mesh resolution and can have slowing down effects on the flow. For instance, this is enhanced in the curbs, which take longer to empty with Mike 21 than with OpenFOAM.

Despite the above-mentioned differences, a good general behaviour agreement is observed, and is reinforced by the calculation of non-trivial quantities, such as surface flow rates. Discharge was computed through Section 1 (Figure 10). This figure enhances the differences in discharge evolution and magnitude which are due to previously explained remarks.

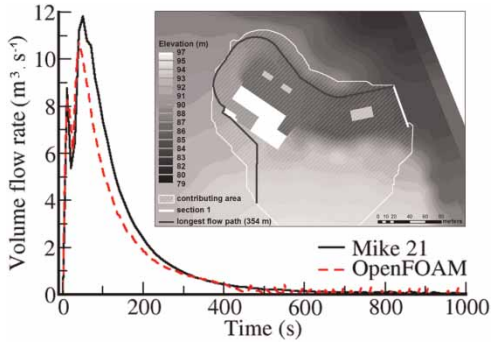

Figure 10 | Hydrograph at Section 1 along with associated upstream contributing area and longest flow path.

Indicators of computation reliability in models

Mass balance

To detect and quantify potential errors in mass, a control of water injected, present and flowing out of the model during the simulation was performed. This mass balance check for scenarios S1a and S1b with Mike 21 FM do not indicate any mass defaults. With Mike 21 mass balance reveals up to a 4% excess in mass at the end of rainfall events ($t = 60$ min for S1a and S1b) reaching 6% after 90 min. For S2 scenarios, the mass error calculation reveals a 2% mass excess with Mike 21. Indeed, it is well known and documented that in the case of steep gradient and small water depth along with spurious oscillation occurrences, calculation can yield negative water depth (DHI 2003). This being the case, Mike 21 automatically resets the water depth to a small positive value, therefore creating mass. In our cases, mass creation appears to be reasonable with Mike 21 and negligible with Mike 21 FM.

Though the OpenFOAM VOF method should be conservative, a 2% default in mass is observed after 30 min of simulation. A fraction of water in cells situated near the atmosphere boundary can be a direct contribution to loss of mass. This phenomenon can be particularly important in the coarse regions of the mesh. Indirect contributions come from numerical diffusions and cumulative errors inherent to the iterative method used (Löhner 2008).

Maximal Courant number (CFL_{max})

For both S1 and S2 categories of scenarios, Mike 21 CFL_{max} values in x and y directions are below 0.2, except for a few cells in curbs where CFL_{max} values can reach 0.3.

With Mike 21 FM, CFL_{max} can be fixed as an input parameter controlling the time steps used in calculations. Fixed CFL_{max} conditions are not overtaken during the various simulations. Nevertheless, in curbs and road gutters, where cell sizes are low and flow velocities higher than for the rest of the domain, time steps were decreased up to 1^{-10} s to keep calculation under imposed CFL conditions. This resulted in drastic computational time increases. The solver used by Néodyme 3D FVM relies on an adaptable time step too, and for a CFL_{max} fixed at 0.5, no instabilities occurred (the time step does not decrease below 10^{-3} s). These differences in time step accommodations with both Mike 21 FM and OpenFOAM are directly related to differences in spatial discretisation resolution.

Maximal velocities (U_{max}) and lag time (T_{lag})

An overview of computed maximal velocities (U_{max}) was performed. For the S1 category of scenarios, computed U_{max} values are up to 3 m s^{-1}, in road curbs and sloping areas. Globally for a given scenario, computed U_{max} values are comparable between models. These flow velocities are in agreement with the magnitude of flow velocities that can be observed for such phenomena in curbs and streets (Ciliberti *et al.* 2008).

For S2 scenarios, the U_{max} range of values is higher. This is due to a high h_{init} value (0.1 m), especially over high topographical gradient areas, and to a higher range of h_{max} values reach in computation. Magnitudes of U_{max} are slightly higher with Néodyme's 3D FVM compared to the Mike 21 model due to differences in roughness energy losses computed in models. No mesh-induced artificial polarisation was detected through evolution of velocity vectors scan for any of the created models.

A check of characteristic times was performed at Section 1 located downstream of our area of interest (Figure 10). Lag time (T_{lag}) and concentration time (T_c) estimated through an empirical approach and through hydrographs extracted from simulation have the same order of magnitude.

DISCUSSION

Comparisons of the results on h_{max} and on indicators of computation reliability performed in this study give an insight on standard modelling tools' possibilities and limits to simulate runoff over an industrial site with high resolution topographical data use. Validations of models through field measurement would have been a reliable approach for confirmation of results and findings, but could not be carried out for this study. Moreover, some parameters and effects treated by 2D SWEs deserve to be more fundamentally studied (eddy and roughness coefficient notably) to see whether the treatment of their influence in models is still valid in this application context and scale. Nevertheless, the implemented approach allows us to point out and enhance some critical aspects.

Discretisation and high topographical gradients

Mike 21 was not the most convenient modelling tool for an adapted spatial discretisation of a domain with detailed small-scale infrastructures. Indeed, compared to unstructured mesh models, it does not offer refinement possibilities around structures in discretisation. Mike 21's software time step lower limit is 0.01 s. This time step restriction in software limits the stable use of a regular spatial discretisation finer than a 0.30 m resolution with a reasonable CFL number for our type of application. In this case, smaller spatial and temporal discretisation would have increased the simulation computational cost, but the gain would not have been relevant, as computed water depths are already comparable to models using a finer discretisation (Mike 21 FM model for instance). Nevertheless, this limit in discretisation possibility might lead to restriction in Mike 21's use for runoff modelling over more complex industrial sites with structures requiring a finer discretisation.

Mike 21 FM is more adapted for fine discretisation of an industrial environment but its numerical scheme cannot handle a high gradient with the same flexibility as does Mike 21. Indeed, high gradient may yield to instabilities leading to computation failure. To overcome this difficulty, BH representations of high topographical gradient structures (buildings, walls, etc.) can be used. Such an approach can be partially automatically treated by Mike

21 FM mesh generator, but still requires time-consuming hand-made operations. Moreover, limits of BH approach use to overcome high gradient generated instabilities were encountered. For instance, the S2-type scenario could not stably run with Mike 21 FM. Indeed, in this case, high gradients leading to numerical instabilities were gradients located along curbs. Curbs are infrastructures that cannot be treated through a BH approach. A mesh refinement optimisation could have partially improved this high gradient issue for the S2 scenario, as well as reduce the computational cost for the S1 type of scenarios, but is a time-consuming task, especially with the actual Mike Mesh generator.

The Néodyme 3D FVM approach allows a fine spatial and temporal discretisation. Nevertheless, it still requires significant work for mesh construction, as well as a significant computational cost. The use of an automated hexahedral meshing tool (e.g., Owens & Saigal 2000) would be the solution to overcome problems that arise when extruding quadrilateral surfaces mesh, because it would facilitate the environmental drawing/meshing, and it would provide better cell shape allowing time steps 10 times larger (or more), thus considerably reducing computational duration. In Néodyme's work, high gradient zones of the topography were filled by hand with locally structured volume meshes. This method requires computer-aided design work, whereas the use of an automated non-structured hexahedral mesh generator would only necessitate drawing of the surfaces (part of the work that could be automated too). Work is in progress in this direction by the Néodyme R&D team.

Flow regime changes treatment

Unsteady flow regime changes are numerically treated in a stable manner by the Mike 21 ADI scheme in the test case under significant CFL number restrictions (<0.2). It confirms Madsen's (2005) conclusion which states that the treatment implemented in Mike 21 to handle trans-critical flow can correctly deal with unsteady flow regime changes only for a CFL number below 0.2. Such restriction leads to a high computational cost, due to low time step used in respect of CFL condition. Moreover, for our scenarios' simulations in the test case, such a low CFL restriction is found to be compulsory in order to have stable runs with small spurious oscillations, as higher time step configurations were tested and led to numerical instabilities. For both Mike 21 FM and Néodyme models, flow regime changes can be handled in a stable manner by numerical schemes involving a high computational cost as well.

Threshold for complete 2D SWEs resolution

Wetting/drying of cells represents a dynamic change of flow domain boundary condition problem, which occurs in the case of high resolution runoff modelling. In both Mike 21 and Mike 21 FM modelling tools, the technique for the treatment of this problem consists of modification of equations' numerical treatment in very shallow regions. With our test case, the Mike 21 numerical method allows a lower h_{wet} value compared to Mike 21 FM for complete SWEs resolution. For both modelling tools, this threshold value, which represents the limit for the start of complete SWEs resolution, can be low enough for the presented practical application purpose. Nevertheless, when cells switch from dry to wet (e.g., throughout the domain when the amount of accumulated rainfall exceeds the h_{wet} value) or vice versa, numerical oscillations are generated. Thus, instabilities might occur, especially with low threshold values. On the other hand, increasing these threshold values leads to more important spurious oscillations (with Mike 21) and to a greater restriction in approach reliability.

Computation reliability

Indicators were checked to spotlight possible inconsistencies in computation and results. These indicators did not indicate major defaults in computation and even if it was not possible to validate results with measures, values appear to be in accordance with physics of modelled runoff phenomena as well as among models. Nevertheless, in the tested modelling tools, the numerical schemes used are not 'well-balanced' schemes and they do not handle compatibility between numerical flux and source terms. This results in numerically created spurious oscillations. This represents an issue for preserving steady states at rest and to properly handle flooding and drying. Thus, spurious oscillations, mass creation and instabilities might occur with standard numerical tools used for such applications.

Checking these computation reliability markers and keeping them under an acceptable level is compulsory and requires modeller expertise. These checks condition high resolution runoff modelling relevance itself and impact upon numerical uncertainty significance.

CONCLUSIONS

The need of high resolution modelling is clearly increasing in the urban and industrial sectors. Stakeholders wish to assess accurately the potential of flood risk due to intense runoff and evaluate the damage to equipment and infrastructures in order to increase resilience. This new task represents a significant challenge for modelling tools commonly used in practical application studies, which have not been designed for handling such processes and spatial scales. In order to assess their performance and limits for surface runoff modelling over an industrial site test case, a selection of standard modelling tools (Mike 21, Mike 21 FM, OpenFOAM) has been tested. Therefore, a pragmatic methodology for such a high resolution modelling purpose has been investigated. A proof of concept of such an approach is enhanced in this paper.

Regardless of the tested modelling tools' numerical methods, simulated water depth evolutions and maximal water depth estimations are comparable among models for a given scenario. Indeed, the tested numerical modelling tools can comparably perform a few centimetres height runoff event simulation on a high resolution topography representing a few centimetres surface drainage influencing infrastructures (pavements, curbs, doors steps, etc.). Results have not highlighted major failures in calculation through mass balance, CFL number, oscillations, velocities and lag time check. Nevertheless, cautions regarding the approach are given: first, regarding the validity of empirical friction law used in the selected modelling tools which would require further research for application for our specific purpose; second, concerning numerical difficulties encountered by standard models due to high gradient occurrences, flow regime changes and wetting/drying moving boundaries treatment. If no attention is paid to these, the difficulties might lead to unstable computation or to biased water depth estimations.

Overcoming these numerical difficulties is possible, but requires an important effort in model optimisation, which in the case of an engineering practical application perspective relies on tools' possibilities and the options available for parameterisation. Optimisations in computation were performed and common difficulties for an optimal model building with standard tools for our specific application were raised and were mainly a function of:

1. possibilities in discretisation refinement;
2. degree of flexibility in numerical treatments to accommodate flow regime changes and high gradient treatment;
3. inherent limitations to obtain an adapted threshold for complete 2D SWEs resolution.

Indeed, critical aspects to achieve an equilibrated balance between computational stability, both swift and precise were emphasised. To estimate the computation reliability of models for such application, at least, indications such as maximum CFL number, mass balance check and spurious oscillation occurrences in results should be carefully regarded.

REFERENCES

Aktaruzzaman, M. & Schmidtt, T. 2009 Detailed Digital Surface Model (DSM) Generation and Automatic Object Detection to Facilitate Modelling of Urban Flooding. ISPRS Workshop, Hannover.

Bidmon, K. & Thomas, E. 2005 Generation of mesh variants via volumetrical representation and subsequent mesh optimisation. *Proceedings, 14th International Meshing Roundtable*, Springer-Verlag, San Diego, CA, pp. 275–286, September 2005.

Ciliberti, S. A., Gomez, M., Macchione, F., Russo, B. & Villanueva, A. 2008 2D analysis for local flooding assessment in a new square of Barcelona during storm events. *11th International Conference on Urban Drainage*, Edinburgh, Scotland, UK, p. 9.

DHI 2003 *Hints and Recommendation in Application with Significant Flooding and Drying*. Danish Hydraulic Institute, Horsholm, Denmark, p. 8.

DHI 2007a *MIKE 21 FLOW MODEL, Hydrodynamic Module: Scientific Documentation*. Danish Hydraulics Institute, Horsholm, p. 58.

DHI 2007b *MIKE 21 & MIKE 3 FLOW MODEL FM, Hydrodynamic and Transport Module: Scientific Documentation*. Danish Hydraulics Institute, Horsholm, p. 50.

Ettrich, N. 2005 Generation of Surface Elevation Models for Urban Drainage Simulation. Bericht des Fraunhofer ITWM, No. 79, p. 29.

Geuzaine, C. & Remacle, J.-F. 2009 Gmsh: a three-dimensional finite element mesh generator with built-in pre- and post-processing facilities. *Int. J. Numer. Meth. Eng.* **79** (11), 1309–1331.

Gomez, M., Macchione, F. & Russo, B. 2011 Methodologies to study the surface hydraulic behaviour of urban catchments during storm events. *Water Sci. Technol.* **63** (11), 2666–2673.

Gopala, V. R. & Wachem, B. G. M. 2008 Volume of fluid methods for immiscible-fluid and free-surface flows. *Chem. Eng. J.* **141**, 204–221.

Gourbesville, P. 2009 Data and hydroinformatics: new possibilities and challenges. *J. Hydroinformat.* **11** (3–4), 330–343.

Gourbesville, P., Pisot, N., Le Fur, H. & Linberg, S. 2004 High resolution digital elevation models: a major interest for urban flooding management. *6th International Conference on Hydroinformatics*, Singapore, pp. 621–629.

Henrik, R. 2002 Computational Fluid Dynamics of Dispersed Two-Phase Flows at High Phase Fractions. PhD Thesis, Department of Mechanical Engineering, Imperial College, London, pp. 343.

Hrvoje, J. 1996 Error Analysis and Estimation for the Finite Volume Method with Applications to Fluid Flows. PhD Thesis, Department of Mechanical Engineering, Imperial College, London, pp. 343.

Lax, P. D. & Wendroff, B. 1960 Systems of conservation laws. *Commun. Pure Appl Math.* **13** (2), 217–237.

Liang, D., Lin, B. & Falconer, R. A. 2006 A boundary-fitted numerical model for flood routing with shock-capturing capability. *J. Hydrol.* **332**, 477–486.

Löhner, R. 2008 *Applied Computational Fluid Dynamics Techniques*, 2nd ed. John Wiley & Sons, Chichester, p. 433.

Madsen, P. A., Simonsen, H. J. & Pan, C.-H. 2005 Numerical simulation of tidal bores and hydraulic jumps. *Coast. Eng.* **52**, 409–433.

Mark, O., Weesakul, S., Apirumanekul, C., Boonya-Aroonnet, S. & Djordjević, S. 2004 Potential and limitations of 1D modelling of urban flooding. *J. Hydrol.* **299** (3–4), 284–299.

McCowan, A. D., Rasmussen, E. B. & Berg, P. 2001 Improving the performance of a two-dimensional hydraulic model for floodplain applications. In: *Conference on Hydraulics in Civil Engineering*, Hobart, Tasmania, p. 11.

Menter, F. R. 1993 Zonal two equation k-omega turbulence models for aerodynamic flows. Nasa Technical Reports Server, AIAA Paper 93–2906.

Meselhe, E. A. & Holly, F. M. 1997 Invalidity of Preissmann scheme for transcritical flow. *J. Hydraulic Engng.* **123** (7), 652–655.

Nikuradse, J. 1933 Laws of flow in rough pipes. VDI Forschungsheft 361. In translation, NACA TM 1292, 1950.

Owen, S. J. & Saigal, S. 2000 H-Morph: an indirect approach to advancing front hex meshing. *Int. J. Numer. Meth. Eng.* **49**, 289–312.

Remondino, F., Barazzatti, L., Nex, F., Scaioni, M. & Sarazzi, D. 2011 Photogrammetry for mapping and 3D modelling – Current status and future perspectives. *International Archives of the Photogrammetry, Remote Sensing and Spatial Information Sciences, Vol. XXXVIII-1/C22, Conference on Unmanned Aerial Vehicle in Geomatics*, Zurich, Switzerland.

Schubert, J. E., Sanders, B. F., Smith, M. J. & Wright, N. G. 2008 Unstructured mesh generation and land cover-based resistance for hydrodynamic modelling of urban flooding. *Adv. Water Resour.* **31**, 1603–1621.

Tsubaki, R. & Fujita, I. 2010 Unstructured grid generation using LiDAR data for urban flood inundation modelling. *Hydrol. Process.* **24**, 1404–1420.

Versteeg, H. K. & Malalasekera, W. 2007 *An Introduction to Computational Fluid Dynamics, The Finite Volume Method*, 2nd edn. Pearson, Harlow, UK.

First received 23 March 2012; accepted in revised form 18 February 2013. Available online 20 March 2013